

Spatial Macroscopic Models of a Bio-Inspired Robotic Swarm Algorithm

Heiko Hamann, Heinz Wörn, Karl Crailsheim, Thomas Schmickl

Abstract— We present a comparative study of two spatially resolved macroscopic models of an autonomous robotic swarm. In previous experiments, the collective behavior of 15 autonomous swarm robots, driven by a simple bio-inspired control algorithm, was investigated: In two different environmental conditions, the ability of the robots to aggregate below a light source was tested. Distinct approaches to predict the dynamics of the spatial distribution were made by two different modeling approaches: One model was constructed in a compartmental manner (ODEs). In parallel, a space-continuous model (PDEs) was constructed. Both models show a high degree of similarity concerning the modeling of concrete environmental factors (light), but due to their different basic approaches, show also significant differences in their implementation. However, the predictions of both models compare well to the observed behavior of the robotic swarm, thus both models can be used to develop further extensions of the algorithm as well as different experimental setups without the need to run extensive real robotic preliminary experiments.

I. INTRODUCTION

In swarm robotics, a group of robots performs a joint task collectively. Usually, the control algorithms are simple and complexity is mainly achieved through robot-to-robot interactions. To analyze the underlying principles and to improve the swarm, a modeling approach allows to investigate its performance in a variety of environmental conditions as well as the effects of different parameters. Models of multi-agent systems can be classified according to the representation of the individual agent. If an agent is explicitly modeled the model is called microscopic. If an agent is only represented by ensembles of agents, for example agent densities, the model is called macroscopic. The main advantages of such macroscopic modeling approaches are twofold: First, simulation is much faster than real world hardware experiments, thus a much bigger variety of conditions can be investigated. Second, modeling abstraction can reveal the core components (constraints, feedback loops) causing the behavior of the swarm. This is mainly due to the omission of irrelevant microscopic details [10]. Thus, abstract modeling and comparison of simulation results to real world experiments can significantly enhance the understanding of the main processes ‘steering’ the robotic swarm. This is why macroscopic modeling approaches, such as the rate equation approach [8], [3] and others [11], [7], are the state-of-the-art modeling techniques in swarm robotics. While simple differential equations can suffice to model, e.g. behavioral

H. Hamann and H. Wörn are with the Institute for Process Control and Robotics, Universität Karlsruhe (TH), 76131 Karlsruhe, Germany {hamann, woern}@ira.uka.de

T. Schmickl and K. Crailsheim are with the Department for Zoology, Karl-Franzens-Universität Graz, Graz, Austria {karl.crailsheim, thomas.schmickl}@uni-graz.at

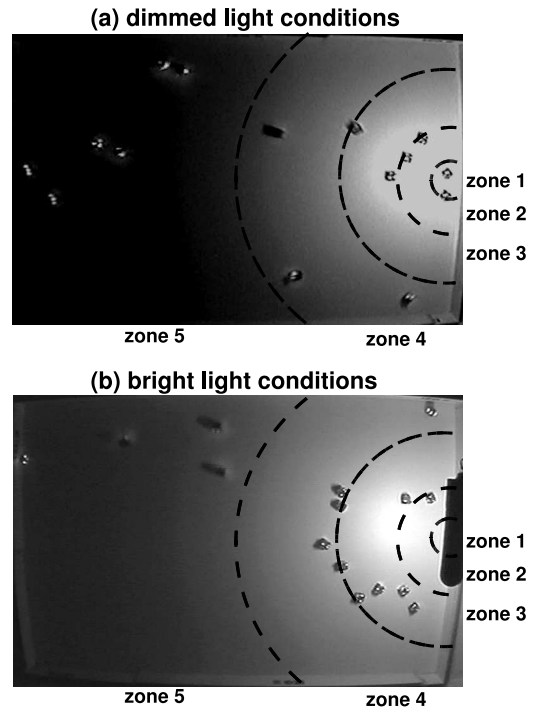


Fig. 1. Frames taken by the tracking video camera mounted above the arena during the robotic experiments, showing the typical results: In bright light conditions, more robots aggregate below the lamp (right side of arena) than in dimmed light conditions. With bright light, more robots form (often ring-shaped) clusters at the peripheral area of the light spot. With dimmed light, robot clusters are formed more in the center of the light spot.

states of robots [9], one important key feature of a robotic swarm is the spatial distribution of its members. Thus, there is a demand for spatially-explicit macroscopic models.

II. INVESTIGATED ROBOTIC SWARM SCENARIO

In the work presented here, we demonstrate how two different approaches towards such a spatial macroscopic model can be made. As a focal example, we took the collective behavior of a swarm of 15 Jasmine robots navigating by the BEECLUST algorithm¹ in an arena of 150 cm × 100 cm. This robotic algorithm can be classified as being swarm-intelligent [2], [1]. The arena is lighted by a lamp from one side, the luminance of this lamp was modulated in two steps: dimmed (about 390 lux at the center of the light spot) and bright (1100 lux).

The robots’ behavior is as follows:

¹The BEECLUST algorithm is inspired by the behavior honeybees show when they aggregate around a spot with optimal temperature [6].

- 1) Robots basically move straight. If they approach an obstacle, they stop and continue with step 2.
- 2) Robots check whether or not the obstacle is another robot by looking for emitted IR signals. If the obstacles emit such signals, they are other robots and the robot continues with step 4. If the obstacles do not emit IR signals, they are arena walls and the robots continue with step 3.
- 3) Robots turn away from the obstacle. As soon as they have no other obstacles in front, they continue with step 1.
- 4) Robots measure the local luminance. The higher this local luminance is, the longer they stay motionless on the place. After the waiting period is over, they turn 180 degrees and continue with step 1.

This simple behavioral algorithm leads to collective aggregation of robots below the light source. The intensity of the light influences the total number of robots that aggregate below the light source [9]. Besides that, also the spatial pattern of aggregated robots at the light source changes with different intensities of the light: With dimmed light, fewer robots aggregate at the light source, but these robots approach the center of the light spot closer. With brighter light intensity, more robots aggregate, but approach the center of the spot less precise.

III. MACROSCOPIC MODELING ASSUMPTIONS

In our modeling approaches, we interpreted the robots as randomly moving units resembling molecules in Brownian motion. Although robots typically turn away from regions of higher densities heading towards less populated areas as in diffusion processes, this is a rather rough simplification which is discussed in the last section.

In the following we propose two models: a ‘compartment’ model based on ordinary differential equations (ODE) with an explicit discretization of space and a model based on partial differential equations (PDE) with continuous space but, in fact, an implicit discretization due to the numerical solver. Thus, in both models we define equations for discrete zones describing the in- and outflow of robots, i.e. robot fractions.

In both models we use the same functions and parameters for the light distribution, the same functions to model the sensors, the same calculation of the waiting time, etc. It is crucial to accurately calculate the expected number of collisions for a certain number (or density) of free and aggregated robots. For this purpose we apply simple collision theory [13]. First, consider the situation of a free robot f moving at velocity v and passing an area occupied by aggregated robots. Robot f covers a distance of $v\Delta t$ in a time of Δt and collides with an aggregated robot a if $\text{dist}(f, a) \leq r$, for the avoidance radius r . Thus, the relevant area covered by a free robot is

$$C_{f,a} = 2rv. \quad (1)$$

By multiplying $C_{f,a}$ with the number of aggregated robots in a considered area divided by the size of this area, i.e. a

density of aggregated robots, we get the number of expected collisions for a single free robot.

Second, consider the situation of a free robot f passing an area populated by other free robots, all moving at the same velocity v . Now, we have to take the relative speed into account. For example, two robots traveling in the same direction keep their distance and do not collide, while others heading for confrontation collide within a short time. This is accounted for by summing the relative speeds over all uniformly distributed velocity vector configurations resulting in $\frac{4v}{\pi}$. By using this mean relative speed instead of v we get the equivalent of eq. 1 for free-to-free collisions:

$$C_{f,f} = r \frac{4v}{\pi}. \quad (2)$$

By multiplying with the density of free robots we get the expected number of colliding robots which is twice the number of collisions.

In the following part we present the ODE-based model followed by the PDE-based model.

IV. THE COMPARTMENT MODEL

In a first approach towards a spatially explicit macroscopic model, we took the approach of compartment models [12], which is rather similar to stock-and-flow models (used in ‘system dynamics’ [4]). The basic concept in compartmental models is, that the system is discretized in several compartments which exchange material via inflows and outflows. Compartmental models are frequently used in physiology to model the flow of chemicals between cell compartments or body compartments. We used this approach to model the flow of robots between certain zones in the arena. The arena was subdivided by concentric rings organized around the central zone below the light spot, which is the area with the highest local luminance. The basic modeling steps are described as follows (see also Fig. 2):

- 1) Robots can move from each zone (ring) only to the two neighboring zones, despite the outermost and the innermost zone, which only have one neighboring zone. These flows of robots among zones are described by the rates $\delta_{i,j}$.
- 2) Robots can approach other robots with a given likelihood, determined by the local density of robots inside of each zone. This is expressed by the rates α_i .
- 3) Robots start to move again depending on the median local luminance that is present in the given zone, as expressed by the rate β_i .

Fig. 2 shows the basic scheme of this modeling approach. In the model that was finally simulated, the arena was organized in 5 distinct zones: The central circular zone at the brightest spot with a radius of $R_1 = 11\text{cm}$. Three ring-shaped zones with radii $R_2 = 22\text{cm}$, $R_3 = 33\text{cm}$, and $R_4 = 66\text{cm}$. The fifth zone covered the remaining area of the arena, which had the dimension of $150\text{ cm} \times 100\text{ cm}$.

In our model, the number of free driving robots in each zone i is expressed by the variable $F_i(t)$, whereas the number of aggregated (stopped) robots is expressed by the variable

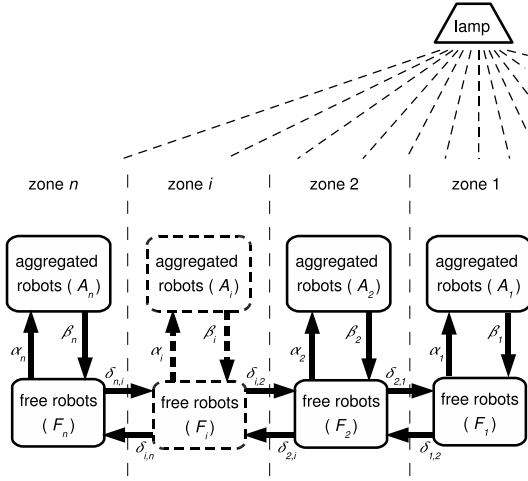


Fig. 2. The first model is organized in a compartmental manner: A chain of linked zones, which represent concentric ring-shaped or disc-shaped zones in the robot arena. Inside of each compartment, robots can switch from the driving state to the stopped (aggregated) state and vice versa.

$A_i(t)$. Robots leave a focal zone i with the rates $\delta_{i,i+1}$ and $\delta_{i,i-1}$ (except the two end zones in the chain). In parallel, robots enter a focal zone with the rates $\delta_{i+1,i}$ and $\delta_{i-1,i}$. These rates of flow are modeled as

$$\delta_{i,i-1}(t) = 0.5vDF_i(t) \frac{R_{i-1}}{(R_i + R_{i-1})(R_i - R_{i-1})}, \quad (3)$$

whereby v represents the average speed of robots, $D = 0.5$ is a diffusion coefficient, which is correlated with the degree of randomness in robot motion (caused by the robot-to-robot collision avoidance as well as wall avoidance). $\frac{R_{i-1}}{R_i + R_{i-1}}$ expresses the proportion of length of the two arc segments that form the borders to the neighboring zones. If these two arcs were of equal length, half of the robots would pass on average to one side and half of the robots would pass to the other side. $(R_i - R_{i-1})$ expresses the width of the zone as it is defined by the difference of the two radii (R_i and R_{i-1}).

For the innermost zone, which is the one directly beneath the center of the lamp, the equation gets simplified, as robots can just leave into one direction. Because the lamp in our empiric experiments was mounted above the side wall of the arena, zone 1 is shaped like a half disk and the zones 2 and 3 are shaped like half-ring segments. The zones 4 and 5 have more complex shapes, due to the fact that the arena was rectangular and the light spot was of circular shape. The rate with which robots leave the central zone 1 is

$$\delta_{1,2}(t) = \frac{vDF_1(t)}{R_1}. \quad (4)$$

Also the outermost zone had to be modeled specially, as described by

$$\delta_{5,4}(t) = \frac{vDF_5(t)}{l_{arena} - R_4}, \quad (5)$$

for the length of the arena $l_{arena} = 150cm$.

Within each zone, robots aggregate to clusters, as soon as they encounter other robots. Thus the collision frequency of robots depends on the number of driving robots and on the number of already aggregated robots inside of this zone. This distinction is necessary, because there is a difference of probability to meet driving robots and standing robots, as is already explained in eq. 1 and 2. The two coefficients $C_{f,a}$ and $C_{f,f}$ express these two different likelihoods. The parameter P_{detect} is the probability that a robot recognizes another robot and can discriminate it from the arena wall. C_i represents the area of the focal zone i (in cm^2). The aggregation rate in each zone i is

$$\alpha_i(t) = F_i(t)P_{detect} \frac{C_{f,a}A_i(t) + C_{f,f}F_i(t)}{C_i}. \quad (6)$$

The rate robots leave clusters in a zone i is described as (β_i). This rate depends on the waiting time of robots, which in turn correlates with the local luminance at the place where the robot initially encountered the cluster. In our model, we used the average luminance of the zone for all robots that form clusters within this zone. This simplification was necessary because of our discretization of the arena space. As it was implemented in the robots' control algorithm, the relationship of waiting time (w) in the zone i to the local luminance (E) was non-linear: Each robot maps the local luminance E in a linear manner to a sensor value reported from its luminance sensor (e), which was in turn used to determine the waiting time w for the robot in a sigmoid manner, as described with eq. 7. Due to the discretization of our model, these variables were treated separately for each compartment i , whereby E_i , e_i , w_i represent the expected luminance, light sensor value and waiting period for all robots located in the center of the zone:

$$w_i = \max \left(1, \frac{w_{max}e_i^2}{e_i^2 + \Omega} \right), \quad (7)$$

whereby w_{max} refers to the maximum waiting time a robot should wait with maximum local luminance. Eq. 7 always converges to w_{max} . The parameter Ω models how fast the waiting time w_i approaches w_{max} with increasing local luminance. From practical experiments with our lamp setup, we used $\Omega = 7000$ in our robot implementation and thus we used this value also in our models described here. To avoid division by 0, the waiting time was restricted to values of equal to 1 or above, what reflects also the minimum stay-together-time of robots that meet in totally dark areas of the arena. The rate at which robots leave clusters is directly proportional to the number of clustered robots in the focal zone A_i and to the waiting time of robots in that zone w_i :

$$\beta_i(t) = \frac{A_i(t)}{w_i}. \quad (8)$$

The above equations can now be combined to the final differential equations of our model, describing the changes over time of aggregated (10) and free driving (9) robots in the compartment (zone) i :

$$\frac{dF_i(t)}{dt} = \delta_{i-1,i}(t) + \delta_{i+1,i}(t) - \delta_{i,i-1}(t) - \delta_{i,i+1}(t) - \alpha_i(t) + \beta_i(t). \quad (9)$$

For the rightmost compartment at the end of the chain $i = 1$ we set $\forall t : \delta_{i-1,i}(t) = \delta_{i,i-1}(t) = 0$. Consequently, for the leftmost compartment at the end of the chain i_{max} we set $\forall t : \delta_{i+1,i}(t) = \delta_{i,i+1}(t) = 0$ for all time. The number of aggregated robots within each zone i is modeled by

$$\frac{dA_i(t)}{dt} = \alpha_i(t) - \beta_i(t). \quad (10)$$

V. THE SPACE-CONTINUOUS MODEL

In this model we chose a complete representation of space by modeling it continuously using PDE. This approach of modeling multi-agent systems was taken before in several studies [10], [5]. The robots were represented as (particle) densities by F (free) and A (aggregated). The product $F(\mathbf{x}, t) dx_1 dx_2$ determines the number of robots that are expected to be encountered at position \mathbf{x} within the rectangle of dimensions dx_1 by dx_2 at time t . Following the visualization of the compartment model (Fig. 2) one might find it useful to still think in in- and outflows. This happens in three dimensions. The first two dimensions are due to the robot motion in the plane. Following our model assumptions this was modeled by a diffusion term $D\nabla^2 F(\mathbf{x}, t)$ for a diffusion constant D . The third dimension is time. Free robots are flowing out of $F(\mathbf{x}, t)$, because they aggregate, and they are flowing in because they wake up and move again. This was modeled by introducing a stopping rate $s(\mathbf{x}, t)$ depending on the number of collisions and detection rates as discussed below. The inflow by awaking robots at spot \mathbf{x} and time t is determined by the fraction of robots that stopped at time $t - w(\mathbf{x})$. w is the waiting time similarly defined as in eq. 7 but with luminance sensor values e depending on points in the plane \mathbf{x} . Hence, we got

$$\frac{\partial F(\mathbf{x}, t)}{\partial t} = D\nabla^2 F(\mathbf{x}, t) - s(\mathbf{x}, t)F(\mathbf{x}, t) + s(\mathbf{x}, t - w(\mathbf{x}))F(\mathbf{x}, t - w(\mathbf{x})). \quad (11)$$

Additionally, a PDE for A can be formulated although it is not necessary as the densities of aggregated robots are implicitly defined by F and w . For A we got

$$\frac{\partial A(\mathbf{x}, t)}{\partial t} = s(\mathbf{x}, t)F(\mathbf{x}, t) - s(\mathbf{x}, t - w(\mathbf{x}))F(\mathbf{x}, t - w(\mathbf{x})). \quad (12)$$

An intuitive approach towards understanding these equations is to look at their discretization in parallel to Fig. 2. In Fig. 3 we show the in- and outflow of the patch at position \mathbf{c} in the case of space being discretized by a grid. The flow to and from the neighborhood is determined by the diffusion term $D\nabla^2 F(\mathbf{x}, t)$ in eq. 11. A (simplified) discretization of the Laplace operator ∇^2 using finite differences is

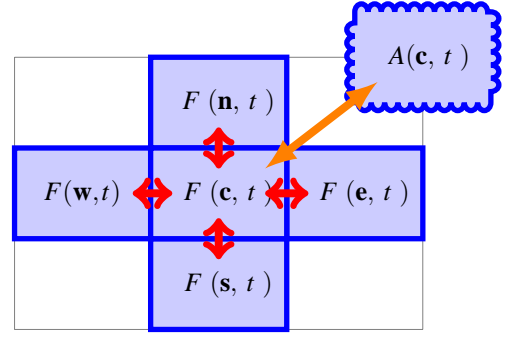


Fig. 3. Schematic diagram of a simple discretization of eq. 11 focusing on one patch in the center (density of free robots at position \mathbf{c} : $F(\mathbf{c}, t)$) and its neighbors to the north, east, south, and west, plus the associated patch of the aggregated robot density $A(\mathbf{c}, t)$. Arrows indicate the in- and outflow.

$$\nabla^2 F(\mathbf{c}, t) \doteq D(F(\mathbf{n}, t) + F(\mathbf{e}, t) + F(\mathbf{s}, t) + F(\mathbf{w}, t) - 4F(\mathbf{c}, t)). \quad (13)$$

Thus, in our model robots tend to homogenize the density in space by leaving areas of high density and accumulating in areas of low density.

Another flow is indicated in Fig. 3 by the diagonal arrow. These are the robots leaving patch \mathbf{c} , because they detected a collision and start waiting, or entering patch \mathbf{c} because their waiting time elapsed. One can think of the patch labeled by $A(\mathbf{c})$ being part of a second grid for the aggregated robots. However, it is rather virtual because the aggregated robots can be administrated by using time-delays and F : Robots are just removed from $F(\mathbf{c})$ for their waiting time w and subsequently returned.

The stopping rate s was derived by using simple collision theory [13] as suggested above. At first, we computed the collision density $Z_{f,a}$ (collisions per time and area) for free robots colliding with aggregated robots. The relevant area as introduced above is $C_{f,a} = 2rv$ (eq. 1). This area is populated by $C_{f,a}A$ aggregated robots giving also the number of expected collisions for a single free robot. Multiplying by F gives the collision density as defined by collision theory

$$Z_{f,a}(\mathbf{x}, t) = C_{f,a}A(\mathbf{x}, t)F(\mathbf{x}, t). \quad (14)$$

The collision density of free robots colliding with free robots was derived by similar considerations except two differences. First, we had to use the mean relative speed leading to an area of $C_{f,f} = r\frac{4v}{\pi}$ (eq. 2). Second, the result needed to be divided by two as each collision is counted twice. We get

$$Z_{f,f}(\mathbf{x}, t) = \frac{1}{2}C_{f,f}F^2(\mathbf{x}, t). \quad (15)$$

The stopping rate is the fraction of free robots, that collide with another robot and detect this collision as well. The probability of detecting a collision successfully is given by P_{detect} which was multiplied to the sum of both collision densities. $Z_{f,f}$ was multiplied by two because each free-to-free collision can potentially convert two free robots into

TABLE I
COMPARISON OF IMPORTANT PARAMETERS USED IN THE MODELS.

Parameter	Compartment Model	Space-Cont. Model
arena dimension	150cm × 100cm	150cm × 100cm
avg. velocity v	30cm/s	30cm/s
avoid. radius r	7.5cm	7.5cm
P_{detect}	0.25	0.25
w_{max}	66	66
diffusion D	0.5	2×10^5
critical density ρ_c	n.a.	$1/(\pi r^2)$

two aggregated robots (this reverts the division by two in the derivation of eq. 15). We got

$$s(\mathbf{x}, t) = \frac{P_{\text{detect}}}{F(\mathbf{x}, t)} (Z_{f,a}(\mathbf{x}, t) + 2Z_{f,f}(\mathbf{x}, t)). \quad (16)$$

Furthermore, we had to introduce a sigmoid function $L(\mathbf{x}, t) \in [0, 1]$ limiting the maximum robot density. It was multiplied to the diffusion D such that it can be interpreted as a space- and time-dependent diffusion. The effect is a slowdown of the robot density flow in regions of high density. We defined

$$L(\mathbf{x}, t) = (1 + \exp(20(F(\mathbf{x}, t) + A(\mathbf{x}, t))/\rho_c - 13))^{-1}, \quad (17)$$

for a ‘critical’ density ρ_c at which the robots’ movements become almost impossible. We chose $\rho_c = 1/(\pi r^2)$. The shape of L , the value of ρ_c , and the diffusion constant D are free parameters that were fitted to the scenario. The boundary conditions were set to total isolation (no robots leave or enter). The initial condition was a homogeneous distribution of robots in the dark half of the arena. We solved eq. 11 numerically (forward integration in time) as the time delay is increasing its complexity critically. It is numerically easy to solve though.

VI. RESULTS AND DISCUSSION

Although many simplifications and modeling assumptions had to be made during the developmental process, both models predicted the spatial distributions of robots in the arena (cf. Fig. 5) extremely well, compared to the empiric results. Even the dynamics of the aggregation in the two peripheral zones (Fig. 4, right column) and in the two central zones (Fig. 4, left column) showed close correlations to the results of the empiric experiments. The high concordance was achieved for both environmental conditions (bright and dimmed light) without any extensive fitting of parameters.

The compartmental model used a very rough discretization of the arena space into 5 compartments. While it was not very difficult to model the process of aggregation (α) and dis-aggregation (β), it was very difficult to model the dispersion of robots in the arena. Especially the heterogeneity of our compartments’ shapes posed a challenge in modeling this diffusion. Both models uses 2 parameters which are hard to determine and which influence the models’ predictions: The diffusion coefficient D and the efficiency of robot-to-robot detection P_{detect} . Both values we used for these two

‘free parameters’ are perfectly within the range of ‘plausible parameters’, as we derived it from our personal observations of robot behavior.

The space-continuous model shows low accuracy in the time-dependent predictions, which is obvious in Fig. 4, bottom right plot. This is induced by assuming a diffusion process. The robots in the experiment showed rather a correlated random walk moving straight between collisions. This time-correlated behavior cannot be modeled macroscopically as mentioned above. The accuracy of the space-continuous model is increased with higher numbers of robots in the experiment, i.e. higher robot density and, thus, the increased collision frequency. For the presented scenario with low density (few robots), the model was adapted by using high diffusion. This leads to a fast ‘mixing’ or homogenization of the density throughout the arena but is a counter-intuitive approach. For even lower robot densities a microscopic approach might prove to be more effective. The other inaccuracy of the space-continuous model is the overestimation of aggregated robots in zone 1. Presumably this is caused by the U-turn behavior described in step 4 of the robot algorithm which is not modeled. By this U-turn, the probability of moving away from the light spot center is higher for a woken up robot than moving towards it.

With both light conditions, the compartmental model was much closer to the observed number of robots in the innermost zone 1, compared to the other model (Fig. 5). Also the dynamics of aggregation predicted by the compartmental model often followed the observed results closely, except in the first 60 seconds, where both models reacted slower than the real robots. Especially with bright light, the dynamics of aggregation in the peripheral zones correspond to the empiric results more closely than the predictions of the space-continuous model (Fig. 4, see bottom-right diagram). On the other hand, the overall distribution of robots in the peripheral zones (last minute of experiments) are predicted by the space-continuous model better than by the compartmental model (Fig. 5)

One major difference between both models is the way how we modeled the process of dis-aggregation. In the compartmental model, we use a simple ‘wake-up’-rate (β) for every zone. In contrast to that, the space-continuous model uses a time-delay function for this process, having the advantage to keep the model structurally simple by omitting separate system variables for aggregated robots. Both models would need additional implementations in the case that the environment (light intensity) were variable over time [9], but this was not necessary for modeling the focal study discussed in this article.

At the end of this study the authors were surprised how closely some parts of the models converged together although the basic modeling approaches were initially very different. The compartmental model was developed in Graz, while the space-continuous model was developed in Karlsruhe simultaneously. So both model approaches shared the same focal empiric study, but represented almost independent modeling processes. Both models had to deal with similar problems in

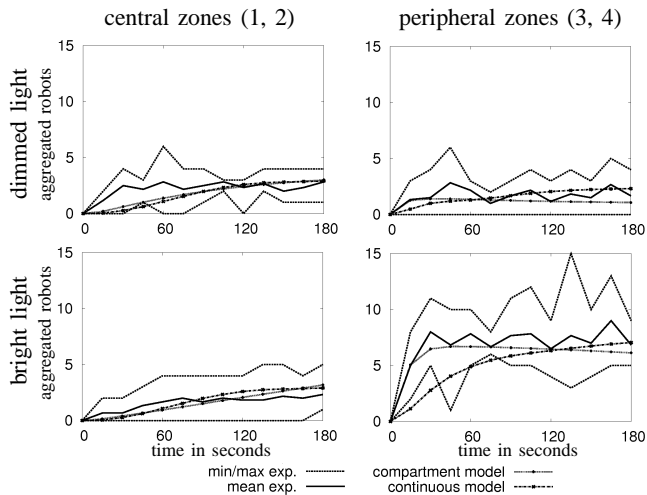


Fig. 4. Comparing the numbers of aggregated robots over time combining the central area (zone 1 and zone 2 pooled) and the peripheral area (zone 3 and zone 4 pooled) of the aggregation place respectively as predicted by the two models to mean, min., and max. of six robot experiments.

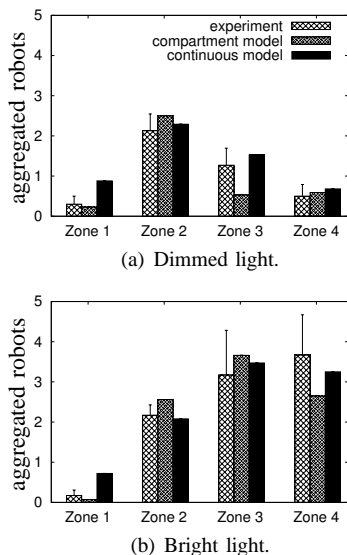


Fig. 5. Comparing the numbers of aggregated robots in each of the four considered zones as predicted by the two models to the mean numbers of aggregated robots in each zone during the last 60 seconds of 6 robotic experiments; error bars indicate upper bound of the 95% confidence interval.

formulating those equations that describe the spatial drift of robots throughout the arena and both models had to formulate the light allocation in the arena. As can be seen in table I, the models converged so closely, that all parameters except D were used with identical values.

VII. CONCLUSION

Our macroscopic approaches only became possible by the simplifying assumption that the robots move randomly similar to a diffusion process. This is a rather rough simplification, as it assumes that collisions happen frequently, thus randomizing robots' directions. However, in our focal experiment, only 15 small robots occupied an arena of

1.5 m^2 . Thus, robots moved in undisturbed and straight (or slightly curved) trajectories for some seconds, executing a 'correlated random walk'. However, modeling this behavior accurately demands for a microscopic model. The consideration of choosing either a microscopic or a macroscopic modeling approach is always a trade-off. The former has a higher accuracy but only for explicit initial configurations (e.g. robot positions, orientations, etc.). Hence, one has to draw many samples from the set of such initializations to get statistically significant results causing a high computational demand. The latter is more abstract, thus exhibits often quantitatively less accurate predictions, but can capture qualitative features ("the dominant main processes") very fast and easy. A macroscopic model can be initialized with an average configuration resulting immediately in predictions of more extensive explanatory power. This is the path we pursued in this paper working on the problem of limited accuracy.

VIII. ACKNOWLEDGMENTS

Hamann is supported by the German Research Foundation (DFG) within the Research Training Group GRK 1194 Self-organizing Sensor-Actuator Networks. Schmickl is supported by the following grants: EU-IST FET project 'I-SWARM', no. 507006 and the FWF research grant no. P19478-B16, EU-IST FET project 'SYMBRION', no. 216342, EU-ICT project 'REPLICATOR', no. 216240.

REFERENCES

- [1] G. Beni. From swarm intelligence to swarm robotics. In E. Şahin and W. M. Spears, editors, *Swarm Robotics – SAB 2004 International Workshop*, volume 3342 of *LNCS*, pages 1–9, Berlin, Heidelberg, 2005. Springer-Verlag.
- [2] G. Beni. and J. Wang. Swarm intelligence in cellular robotic systems. In *Proceedings of the NATO Advanced Workshop on Robots and Biological Systems*, 1989.
- [3] N. Correll. *Coordination schemes for distributed boundary coverage with a swarm of miniature robots: synthesis, analysis and experimental validation*. PhD thesis, Ecole Polyt. Féd. de Lausanne, 2007.
- [4] J. Forrester. *World Dynamics*. Wright-Allen, Cambridge, MS, 1971.
- [5] H. Hamann and H. Wörn. A space- and time-continuous model of self-organizing robot swarms for design support. In *Self-Adaptive and Self-Organizing Systems (SASO'07), Boston, USA*, pages 23–31, 2007.
- [6] H. Heran. Untersuchungen über den Temperatursinn der Honigbiene (*Apis mellifica*) unter besonderer Berücksichtigung der Wahrnehmung von Strahlungswärme. *Zeitschrift für vergleichende Physiologie*, 34:179–207, 1952.
- [7] T. Hogg. Coordinating microscopic robots in viscous fluids. *Autonomous Agents and Multi-Agent Systems*, 14(3):271–305, June 2006.
- [8] K. Lerman, A. Martinoli, and A. Galstyan. A review of probabilistic macroscopic models for swarm robotic systems. In E. Şahin and W. M. Spears, editors, *Swarm Robotics Workshop: State-of-the-art Survey*, pages 143–152. Springer-Verlag, 2005.
- [9] T. Schmickl, H. Hamann, H. Wörn, and K. Crailsheim. Two different approaches to a macroscopic model of a bio-inspired robotic swarm. *Robotics and Autonomous Systems*, submitted.
- [10] F. Schweitzer. *Brownian Agents and Active Particles*. Springer, 2003.
- [11] O. Soysal and E. Şahin. A macroscopic model for self-organized aggregation in swarm robotic systems. In E. Şahin, W. M. Spears, and A. F. Winfield, editors, *Swarm Robotics – Second SAB 2006 International Workshop*, volume 4433 of *LNCS*, pages 27–42, Berlin, Heidelberg, 2007. Springer-Verlag.
- [12] The NSR Physiome Project. <http://www.physiome.org/model/doku.php?id=Tutorials:Compartmental>.
- [13] M. Trautz. Das Gesetz der Reaktionsgeschwindigkeit und der Gleichgewichte in Gasen. Bestätigung der Additivität von Cv-3/2R. Neue Bestimmung der Integrationskonstanten und der Moleküldurchmesser. *Zeitschrift für anorganische und allgemeine Chemie*, 96(1):1–28, 1916.